Available online at www.sciencedirect.com

SciVerse ScienceDirect

Journal of the European Ceramic Society 32 (2012) 2213–2218

www.elsevier.com/locate/jeurceramsoc

A novel way to fabricate highly porous fibrous YSZ ceramics with improved thermal and mechanical properties

Yanhao Dong [a], Chang-An Wang [a,*], Jun Zhou [a], Zhanglian Hong [b,**]

[a] Department of Materials Science and Engineering, State Key Laboratory of New Ceramics and Fine Processing, Tsinghua University, Beijing 100084, China
[b] Department of Materials Science and Engineering, State Key Laboratory of Silicon Materials, Zhejiang University, Hangzhou 310027, PR China

Received 15 December 2011; received in revised form 6 March 2012; accepted 9 March 2012
Available online 1 April 2012

Abstract

Inspired by nest structure, highly porous fibrous yttria-stabilized zirconia (YSZ) ceramics were fabricated through tert-butyl alcohol (TBA)-based gel-casting process and pressureless sintering by using YSZ fibers as raw material and adding K_2SO_4 as removable sintering aid. Different sintering temperature and soaking time were investigated to achieve optimal thermal and mechanical properties. The results show that all specimens consist of crystallized t-YSZ phase. Fibers interconnect with good interfacial bonding on junctions. Under higher sintering temperature, porosity drops gradually while compressive strength increases significantly. With prolonged soaking time, there is no obvious change in porosity and compressive strength increases gradually. All specimens have uniformly distributed pores with average size of 30.2 μm and show good structural stability at high temperature. Ultra-low thermal conductivity is achieved and ductile fracture mode with high elongation makes it more applicable in high-temperature thermal insulating applications.

Keywords: ZrO_2; Fibres; Porosity; Thermal conductivity; Mechanical properties

1. Introduction

Porous YSZ ceramics are potential candidates in thermal insulating applications due to their low density, low thermal conductivity and high temperature resistance.[1–5] Many approaches have been developed to fabricate porous ceramics, including direct foaming,[6,7] template method[8,9] and gel-casting method.[10–12] To further improve the insulating properties, ultra-high porosity and ultra-low thermal conductivity are desired but they are very difficult to achieve especially for porous YSZ ceramics. Nait-Ali et al.[13] used latex as pore former to prepare porous zirconia ceramics with thermal conductivity ranged from 0.13 to 0.55 $W\,m^{-1}\,K^{-1}$. Hu et al.[14] fabricated porous YSZ ceramics by TBA-based gel-casting method with porosity ranged from 75.9% to 51.5% and thermal conductivity ranged from 0.06 to 0.42 $W\,m^{-1}\,K^{-1}$, but the structure is very sensitive to sintering temperature and insulating properties drop with increasing temperature.

Bird's nests are naturally designed structures with both low density and high strength. Branches serve as the components and the structure and properties are critical with the joint bonding between branches. Inspired by this, we proposed to fabricate highly porous ceramics using fibers as the raw material. Here, fibers serve as the components of our desired structure analogically. This fibrous nest-like structure can be obtained by jointing together of fibers through adhering of cements or diffusion bonding. Former approaches used cement adhesion technology,[15,16] but they are unusable at high temperature because of the low melting point of the cement. Therefore, methods to modify are of great urgency to achieve high temperature applications. Molten salt method provides a good approach, in which molten salt offers a unique liquid circumstance for diffusion binding of fiber contact junctions at a proper temperature.

Molten salt method has a long history and has been widely used in metallurgy, electrochemistry, nuclear and energy technology,[17,18] providing a unique liquid circumstance for catalysis, reactions, heat and mass transfer.[19] In this paper, we combined molten salt method with porous ceramics processing

* Corresponding author. Tel.: +86 10 62785488; fax: +86 10 62785488.
** Corresponding author. Tel.: +86 571 87951234; fax: +86 571 87951234.
E-mail addresses: wangca@tsinghua.edu.cn (C.-A. Wang), hong_zhanglian@zju.edu.cn (Z. Hong).

0955-2219/$ – see front matter © 2012 Elsevier Ltd. All rights reserved.
doi:10.1016/j.jeurceramsoc.2012.03.016

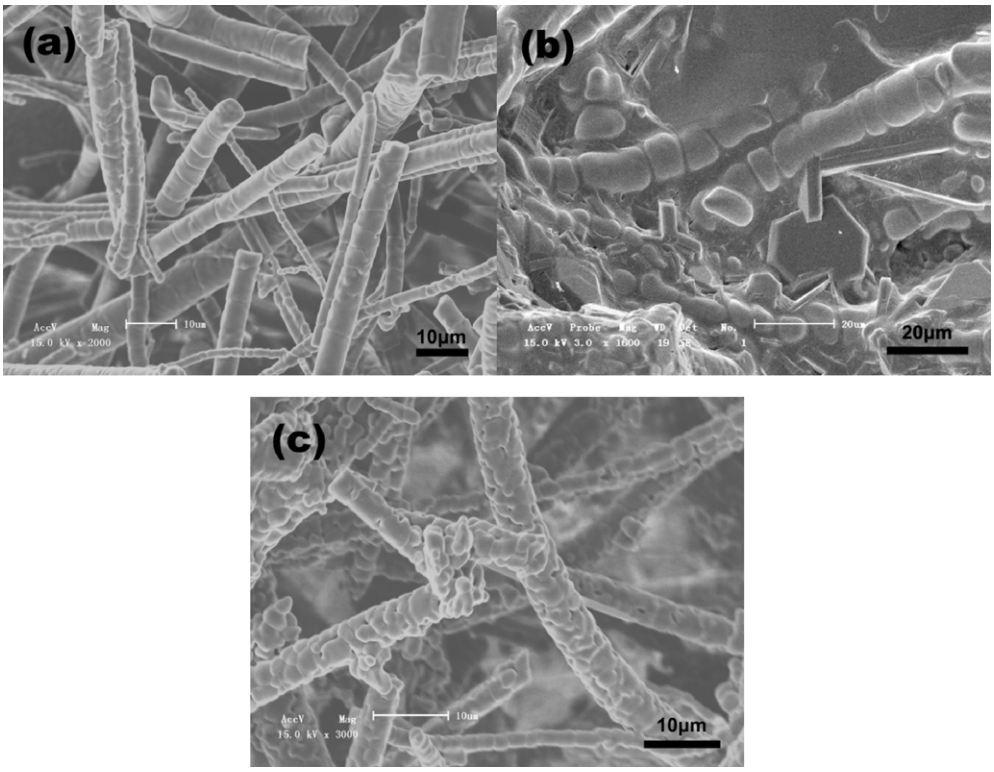

Fig. 1. Microstructure of the specimens with different salt addition, NaCl (a), Na_2SiO_4 (b) and K_2SO_4 (c) sintered at 1600 °C for 2 h.

and developed a novel approach to fabricate highly porous (>85%) fibrous YSZ ceramics with ultra-low thermal conductivity (~0.02 W m^{-1} K^{-1}, lowest ever reported) through TBA-based gel-casting method and pressureless sintering by using YSZ fibers as the raw material and adding K_2SO_4 as removable sintering aid. Here, K_2SO_4 provides a liquid phase above its melting point (1067 °C) at the junctions of YSZ fibers, which promotes the diffusion mass transfer and bonding the YSZ fibers together, while K_2SO_4 will be cleared away by evaporation holding at a higher temperature. Different sintering temperature and soaking time were investigated to achieve optimal porous structure as well as improved thermal and mechanical properties.

2. Experiment procedure

2.1. Materials

Commercially available YSZ fiber (ZrO_2-9 mol%, Shandong High Temperature Fiber Technology Co., Ltd., Hong Zuicho, Shandong, China) was used as the raw material. The YSZ fiber has a smooth surface with a diameter varied from 1 to 10 μm. K_2SO_4 was used as removable sintering aid. Tert-butyl alcohol (TBA, chemical purity, Beijing Yili Chemical Co., Beijing, China) was used as solvent in gel-casting process. BYK163 (BYK-Chemie GmbH, Germany) was used as dispersant. A premix solution of monomers and cross linkers was prepared in TBA with a concentration of 14.5 wt% of acrylamide (AM, $C_2H_3CONH_2$) and 0.5 wt% N,N′-methylenebisacrylamide (MBAM, $(C_2H_3CONH)_2CH_2$). Initiator and catalyst for gelation reaction were ammonium persulfate (APS) and N,N,N,N-tetramethylethylenediamine (TEMED), respectively. All chemicals used in this study are AR grade.

2.2. Fabrication

The TBA-based gel-casting method typically consists of preparing a liquid suspension (slurry), molding, drying, binder removal, and sintering. 24 g YSZ fiber, 10 g K_2SO_4, 4 g BYK163 were added to 76 mL premixed solution to prepare the slurry by ball milling for 30 min with the rate of 250 r/min. After ball milling and deairing, initiator was mixed into the slurry. The slurry was poured into molds and dried at 50 °C in air. During the drying procedure, the polymerization of AM occurred and TBA gradually volatilized. Green bodies were produced and then sintered at different temperature.

2.3. Characterization

Microstructure was observed using scanning electron microscope (SEM, JSM 6700F, JEOL, Tokyo, Japan). Phase composition was analyzed by X-ray diffraction (SHIMAZU S-7000). Pore size distribution was analyzed by the mercury intrusion method (Auto Pore IV 9510). The density and porosity were measured on sintered specimens using the Archimedes method with theoretical density of 6.29 g/cm^3 for the dense YSZ fiber. Compressive strength was measured on CSS-2220 test machine with a crosshead loading speed of 0.5 mm/min. Room temperature thermal conductivity was measured by the Thermal

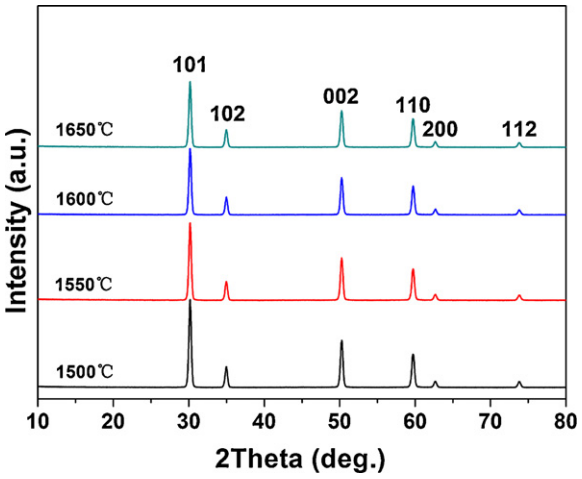

Fig. 2. XRD patterns of the specimens with K_2SO_4 addition sintered at different temperature with soaking time of 2 h.

Transport Option (TTO) of Physical Properties Measurement System (PPMS, Model 6000, Quantum Design, United States).

3. Results and discussion

The sintering mechanism with K_2SO_4 as removable sintering aid is as follows. After drying the gel-cast green bodies and subsequent binder removal, there were only YSZ fibers and K_2SO_4 particles in the specimen. When sintering temperature exceeded the melting point of K_2SO_4 (1067 °C), K_2SO_4 turned into liquid state. Former researches have already shown that the existence of active liquid phase can accelerate mass transfer and thus the whole sintering process.[20,21] Lisinska-Czekaj et al.[22] reported that small amount of molten salt (NaCl) facilitated solid phase reaction of Bi_3NbTiO_9 and lowered the sintering temperature for about 100 °C. In our work, molten K_2SO_4 accelerated diffusion mass transfer between fibers. YSZ transferred to the joints automatically and bonded YSZ fibers together. K_2SO_4 gradually evaporated and then sintered specimens were obtained. In comparison, YSZ fibers without K_2SO_4 addition cannot be effectively sintered (cracks and almost no mechanical strength).

In order to choose an appropriate sintering aid, three kinds of salts, NaCl, Na_2SiO_4 and K_2SO_4, were investigated. Fig. 1(a) shows the details of the morphology of specimens with NaCl addition. Only weak combination can be observed at the joints of YSZ fibers and the mechanical strength of fibrous YSZ ceramics is very low. This is due to the relatively low melting point of NaCl (801 °C) and thus insufficient mass transfer. However, the obtained porosity can be very high (>92%). Microstructure of specimens with Na_2SiO_4 addition is shown in Fig. 1(b). As can be seen, the fiber structure has been destroyed and large amount of Na_2SiO_4 remains in the sintered specimens. Thus Na_2SiO_4 is not a proper choice. Fig. 1(c) is the SEM image of specimens with K_2SO_4 addition. It can be observed that fibers interconnect with each other and grains on the fiber grow up. Good interfacial bonding is shown on junctions as well. Furthermore, the surface topography of fibers and YSZ particles on the junctions confirm the enhanced diffusion mass transfer with the existence of molten K_2SO_4. Therefore, K_2SO_4 is the appropriate choice for molten salt method to prepare porous YSZ ceramics.

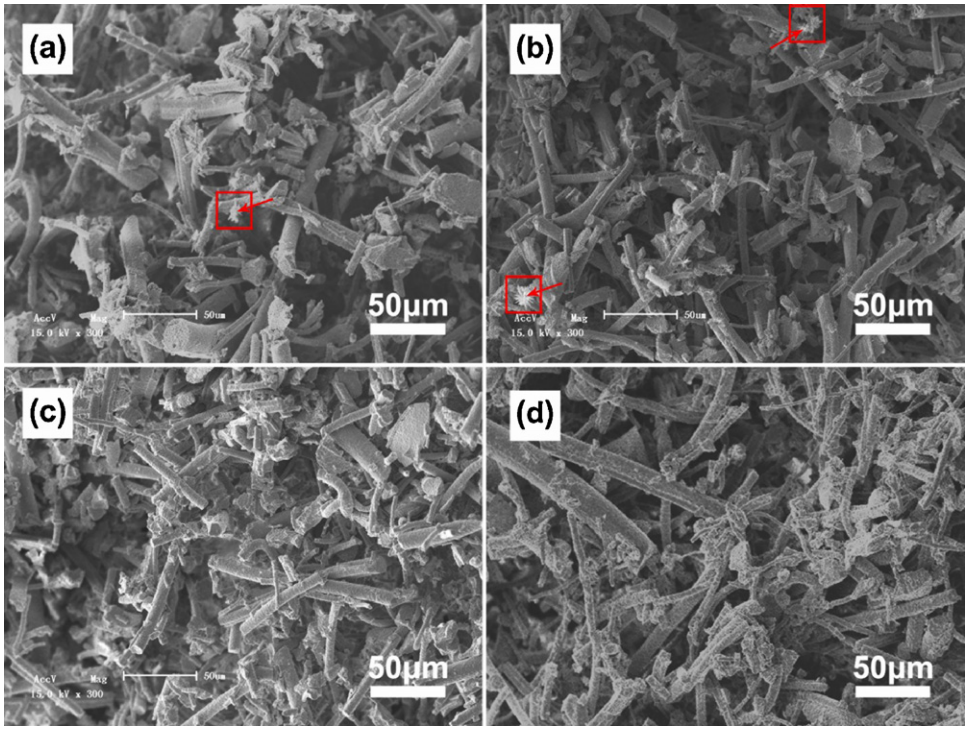

Fig. 3. SEM images of the specimens with K_2SO_4 addition sintered at different temperature, 1500 °C (a), 1550 °C (b), 1600 °C (c), and 1650 °C (d) (arrays in red boxes show the residue of K_2SO_4) with soaking time of 2 h. (For interpretation of the references to color in figure legend, the reader is referred to the web version of the article.)

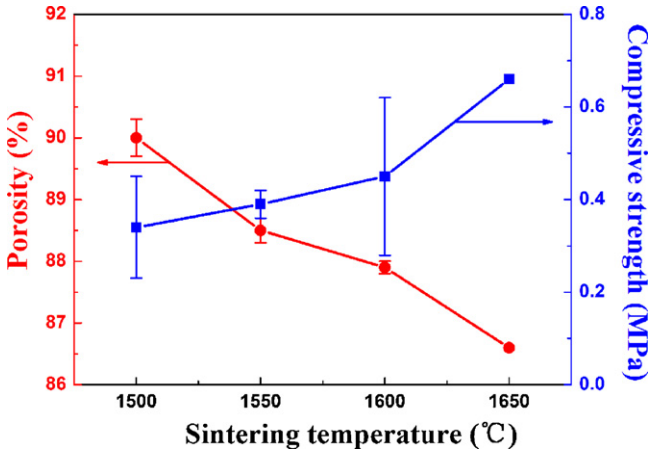

Fig. 4. Variation of porosity and compressive strength of fibrous YSZ ceramics at different sintering temperature with soaking time of 2 h.

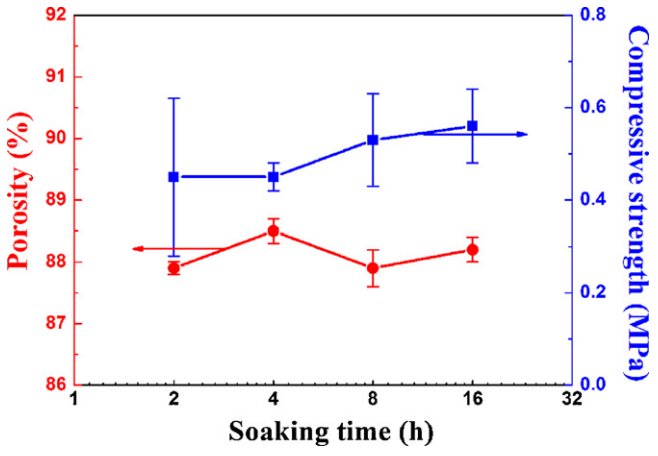

Fig. 5. Variation of porosity and compressive strength of fibrous YSZ ceramics sintered at 1600 °C with different soaking time.

XRD patterns of fibrous YSZ ceramics sintered at different temperature are shown in Fig. 2 with the soaking time of 2 h. The peaks of XRD patterns are very sharp, which indicates good crystallinity. All patterns are well indexed to t-YSZ and no K_2SO_4 phase can be observed. It means that the content of K_2SO_4 is below the detection limit. (Generally, XRD detection is insensitive to content below 5%.) Fig. 3 shows the details of the morphology of specimens with different sintering temperature. As can be seen, they are typical fibrous structures. K_2SO_4 can still be found in SEM images at sintering temperature of 1500 °C and 1550 °C (shown in Fig. 2(a) and (b)) but the amount is minimal. With higher temperature, no K_2SO_4 can be found in SEM images.

Fig. 4 shows the variation of porosity and compressive strength with different sintering temperature (also shown in Table 1). Higher temperature contributes to densification during sintering process. Therefore, porosity decreases gradually while compressive strength significantly increases with increasing sintering temperature. At 1650 °C, the compressive strength increases to 0.66 MPa and we propose that the mechanical strength can be improved with higher sintering temperature; however, no further research is executed due to the limitation of the equipment.

Fig. 5 gives the results of porosity and compressive strength with different soaking time sintered at 1600 °C (also shown in Table 1). When soaking time is extended, there is no significant change on porosity and compressive strength increases gradually, which indicates good stability of structure and properties at high temperature. It is noticed that with higher sintering temperature and prolonged soaking time, there is only small variation on porosity yet the compressive strength is improved. We believe that connections on the joints are the weak parts of the structure and the strength can be further improved with modified joint bonding. During the above process, densification on the joints occurs. It results in better interfacial bonding, which accounts for the increasing strength.

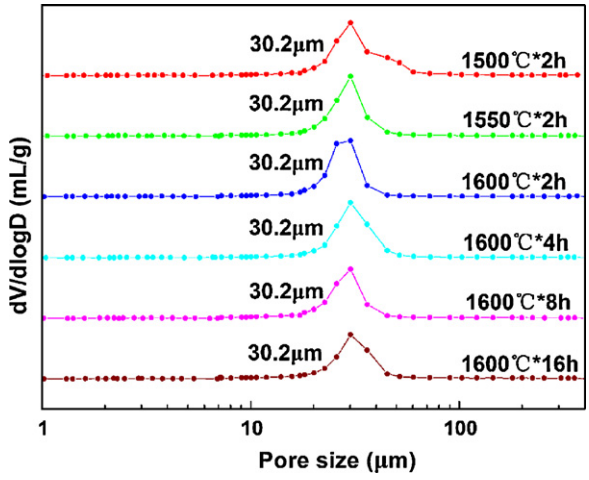

Fig. 6. Pore size distribution of fibrous YSZ ceramics with different sintering temperature and soaking time.

Table 1
Properties of fibrous YSZ ceramics with different sintering temperature and soaking time.

Sintering temperature (°C)	Soaking time (h)	Apparent density (g cm^{-3})	Porosity (%)	Compressive strength (MPa)	Thermal conductivity (W m^{-1} K^{-1})
1500	2	0.63 ± 0.02	90.0 ± 0.3	0.34 ± 0.11	–
1550	2	0.73 ± 0.01	88.5 ± 0.2	0.39 ± 0.03	0.018
1600	2	0.76 ± 0.01	87.9 ± 0.1	0.45 ± 0.17	0.020
	4	0.73 ± 0.01	88.5 ± 0.2	0.45 ± 0.03	0.020
	8	0.76 ± 0.03	87.9 ± 0.3	0.53 ± 0.10	0.027
	16	0.74 ± 0.02	88.2 ± 0.2	0.56 ± 0.08	–
1650	2	0.84	86.6	0.66	–

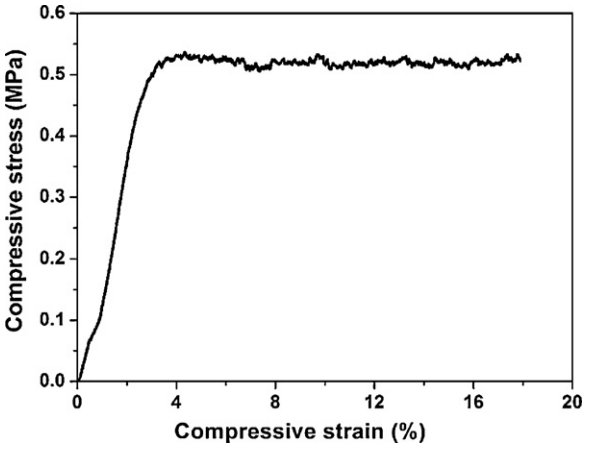

Fig. 7. Compressive strain–stress curve of the specimens sintered at 1650 °C with soaking time of 2 h.

Pore size distributions of specimens with different sintering temperature and soaking time are shown in Fig. 6. Each curve presents a single peak with a narrow width, signifying uniform pore size distributions. All curves show a peak at 30.2 μm, which means that the microstructure is insensitive to sintering temperature and soaking time and indicates good structure stability at high temperature as well.

Typical compressive stress–strain curve of fibrous YSZ ceramics is shown in Fig. 7. Unlike typical brittle fracture mode of ceramics, the fracture mode is a representative ductile one. Compressive stress firstly increases with increasing strain and then shows a very long terrace. Up to 18% strain, there is no declining trend on compressive stress, which indicates large damage tolerance and good reliability in applications. This is because fibers interconnect with each other and share large numbers of joints. Loading force can be transferred and rearranged through fibers and therefore fibrous structure can bear large deflection. Other specimens all have similar compressive stress–strain curves and thus their curves are no shown here for brevity. The stress on the terrace is chosen as compressive strength of the porous YSZ ceramics.

Thermal conductivity data of fibrous YSZ ceramics are shown in Table 1. Ultra-low thermal conductivity ($\sim$0.020 W m^{-1} K^{-1}, lowest ever reported) is achieved, which is even lower than the thermal conductivity of air (0.026 W m^{-1} K^{-1}). This is due to the high porosity and uniformly distributed small pores. Moreover, compared with normal porous ceramics, fibrous structure has longer heat transfer path and thermal resistance on the joint is very large, which enhances photon scatting of the lattice. All these factors contribute to the low thermal conductivity of our specimens. It is noticed that the thermal conductivity of fibrous YSZ ceramics is comparable to silica aerogel yet the structure can maintain stable at higher temperature. Therefore, fibrous YSZ ceramics fabricated in this work show significant advantages in thermal insulating applications at high temperature. Furthermore, fibrous YSZ ceramics can serve as the framework of silica aerogel to improve its mechanical properties, while remaining the ultra-low thermal conductivity.

4. Conclusion

A novel way was developed to fabricate highly porous fibrous YSZ ceramics through TBA-based gel-casting and pressureless sintering by using YSZ fibers as the raw material and adding K_2SO_4 as removable sintering aid. Porosity can be adjusted in the range of 86.6–90.0% with a mean pore size of 30.2 μm. Ultra-low thermal conductivity (0.018–0.027 W m^{-1} K^{-1}) was achieved with a relatively high mechanical strength (0.34–0.66 MPa). Different sintering temperature and soaking time were studied, showing the excellent high-temperature stability of structure and properties, which indicated their good application performance. The ductile fracture mode of fibrous YSZ ceramics with high elongations improved the reliability in applications as well.

Acknowledgment

The authors would like to thank the financial support from the National Natural Science Foundation of China (NSFC – Nos. 90816019, 51172119 and 51102140).

References

1. Vassen R, Cao XQ, Tietz F, Basu D, Stover D. Zirconates as new materials for thermal barrier coatings. *J Am Ceram Soc* 2000;**83**:2023–8.
2. Clarke DR, Phillpot SR. Thermal barrier coating materials. *Mater Today* 2005;**8**:22–9.
3. Zhong XH, Wang YM, Xu ZH, Zhang YF, Zhang JF, Cao XQ. Hot-corrosion behaviors of overlay-clad yttria-stabilized zirconia coatings in contact with vanadate–sulfate salts. *J Eur Ceram Soc* 2010;**6**:1401–8.
4. Saremi M, Afrasiabi A, Kobayashi A. Microstructural analysis of YSZ and YSZ/Al_2O_3 plasma sprayed thermal barrier coatings after high temperature oxidation. *Surf Coat Technol* 2008;**202**:3233–8.
5. Song SH, Xiao P, Weng LQ. Evaluation of microstructural evolution in thermal barrier coatings during thermal cycling using impedance spectroscopy. *J Eur Ceram Soc* 2005;**25**:1167–73.
6. Kishimoto A, Obata M, Asaoka H, Hayashi H. Fabrication of alumina-based ceramic foams utilizing superplasticity. *J Eur Ceram Soc* 2007;**27**:41–5.
7. Wucherer L, Nino JC, Subhash G. Mechanical properties of BaTiO(3) open-porosity foams. *J Eur Ceram Soc* 2009;**29**:1987–93.
8. Rambo CR, Cao J, Sieber H. Preparation and properties of highly porous, biomorphic YSZ ceramics. *Mater Chem Phys* 2004;**87**:345–52.
9. Kim HW, Lee SY, Bae CJ, Noh YJ, Kim HE, Kim HM, Ko JS. Porous ZrO_2 bone scaffold coated with hydroxyapatite with fluorapatite intermediate layer. *Biomaterials* 2003;**24**:3277–84.
10. Chen RF, Huang Y, Wang CA, Qi JQ. Ceramics with ultra low density fabricated by gelcasting: an unconventional view. *J Am Ceram Soc* 2007;**90**:3424–9.
11. Gu YF, Liu XQ, Meng GY, Peng DK. Porous YSZ ceramics by water-based gelcasting. *Ceram Int* 1999;**25**:705–9.
12. Meng GY, Wang HT, Zheng WJ, Liu XQ. Preparation of porous ceramics by gelcasting approach. *Mater Lett* 2000;**45**:224–7.
13. Nait-Ali B, Haberko K, Vesteghem H, Absi J, Smith DS. Thermal conductivity of highly porous zirconia. *J Eur Ceram Soc* 2006;**26**:3567–74.
14. Hu LF, Wang CA, Huang Y. Porous yttria-stabilized zirconia ceramics with ultra-low thermal conductivity. *J Mater Sci* 2010;**45**:3242–6.
15. Hamling BH, Schaffer PC. Applications of lightweight zirconia thermal insulation. *Am Ceram Soc Bull* 1972;**51**:426.
16. Hamling HC, Hamling BH. New forms of zirconia thermal insulation. *Am Ceram Soc Bull* 1984;**63**:1016.
17. Sundermeyer W. Fused salts their use as reaction media. *Angew Chem Int Ed* 1965;**4**:222–38.

18. Dupont J. From molten salts to ionic liquids: a nano journey. *Acc Chem Res* 2011;**44**:1223–31.
19. Descemond M, Brodhag C, Thevenot F, Durand B, Jebrouni M, Roubin M, Characteristics. Sintering behavior of 3 mol percent Y_2O_3–ZrO_2 powders synthesized by reaction in molten salts. *J Mater Sci* 1993;**28**: 2283–8.
20. Kingery WD. Densification during sintering in the presence of a liquid phase. I. Theory. *J Appl Phys* 1959;**30**:301–6.
21. Corker DL, Whatmore RW, Ringgaard E, Wolny WW. Liquid-phase sintering of PZT ceramics. *J Eur Ceram Soc* 2000;**20**:2039–45.
22. Lisinska-Czekaj A, Czekaj D, Gomes MJM, Kuprianov MF. Investigations on the synthesis of Bi_3NbTiO_9 ceramics. *J Eur Ceram Soc* 1999;**19**:969–72.